The Spin Transition of an Iron(III) Complex Intercalated in a $MnPS_3$ Layered Magnet. Occurrence of a Hysteresis Effect on Removal of Lattice Solvent

Sébastien Floquet,[†] Sunita Salunke,[‡] Marie-Laure Boillot,*[,†] René Clément,[†] François Varret,[‡] Kamel Boukheddaden,[‡] and Eric Rivière[†]

Laboratoire de Chimie Inorganique, UMR 8613, Université Paris-Sud, 91405 Orsay, France, and Laboratoire de Magnétisme et d'Optique, UMR 8634, Université de Versailles Saint-Quentin, 78035 Versailles, France

Received February 12, 2002. Revised Manuscript Received June 5, 2002

A cationic iron(III) complex $[Fe^{III}(5\text{-OMe-sal}_2\text{trien})]^+$ (where $[H_2(5\text{-OMe-sal})_2\text{trien}]$ was derived from triethylenetetramine and substituted salicylaldehyde), designed to undergo spin crossover, has been inserted in the layered $MnPS_3$ host lattice. The magnetic properties of the resulting intercalation compound $[Fe(5\text{-OMe-sal}_2\text{trien})]_{0.28}Mn_{0.86}PS_3 \cdot nH_2O$ have been characterized by ^{57}Fe Mössbauer spectrometry and SQUID measurements. The untreated compound exhibits a sluggish thermal spin crossover over the range 200−300 K, but without hysteresis. Removing the co-intercalated water molecules from the compound dramatically affects its behavior and confers a broad hysteresis loop to the transition. The appearance of cooperativity is discussed in terms of elastic interactions and specific arrangement of the ferric complexes. Further interest arises from the spontaneous magnetization acquired by the intercalation compound below 36 K. The static internal magnetic field experienced by the iron sites affects the Mössbauer spectrum of the low-spin form of the inserted complex below T_c.

Introduction

There has been a recent increasing interest in the spin-crossover complexes because of their electronic lability responsible for an extreme sensitivity of their physical properties toward external stimuli.[1−5] This spin-state switching can be driven by temperature, pressure, or light. The magnetic field, whose application results in a Zeeman splitting stabilizing the high-spin state, may also be considered as an efficient control parameter: a quasi-complete triggering of a spin crossover was recently described under the effect of a high pulsed magnetic field.[6,7] In condensed phases, different types of behaviors have been described as the interactions between the spin-crossover molecule and its surroundings (solvent molecule, crystal lattice, or matrix) are varied. In the case where strong cooperative interactions between molecules occur in the solid state, the high-spin (HS) ↔ low-spin (LS) transformation is characterized by the discontinuous variation of different observables (electronic, magnetic, structural, ...). For some of these materials, a first-order phase transition can be identified from a hysteresis effect.

Besides progress in the understanding of thermal spin crossover, light-induced spin switching has extended the scope of investigation to embrace the emerging field of photomagnetism.[5] In the *perspective of designing* new materials possessing some photomagnetic properties,[5,8] we have attempted to build up a nanostructured material assembling molecules, capable of undergoing spin crossover, with specific structural blocks—selected for their own interest.

In the present work, a HS−LS switchable complex is inserted between the slabs of a semiconducting layered host lattice capable of acquiring a spontaneous magnetization. Our goal is not only to assemble two kinds of magnetic properties but also to search for some mutual interactions between them and to identify possible effects of the geometric constraints exerted by the host lattice. More precisely, we report here the thermal spin crossover of a cationic complex $[Fe^{III}(5\text{-OMe-sal}_2\text{trien})]^+$ intercalated in the layered thiophosphate $MnPS_3$ and we present the Mössbauer data that provide evidence for a nuclear spin polarization effect of the low-spin ferric ion caused by the bulk magnetization as well as

* To whom correspondence should be addressed.
[†] Université Paris-Sud.
[‡] Université de Versaillles Saint-Quentin.

(1) Gütlich, P.; Hauser, A.; Spiering, H. *Angew. Chem., Int. Ed. Engl.* **1994**, *33*, 2024.
(2) (a) König, E.; Ritter, G.; Kulshreshtha, S. K. *Chem. Rev.* **1985**, *85*, 219. (b) König, E. *Prog. Inorg. Chem.* **1987**, *35*, 527.
(3) *Molecular magnetism*; Kahn, O., Ed.; VCH Publishers: New York, 1993; p 53.
(4) (a) Bacci, M. *Coord. Chem. Rev.* **1988**, *86*, 245. (b) Toftlund, H. *Coord. Chem. Rev.* **1984**, *94*, 67. (c) Beattie, J. K. *Adv. Inorg. Chem.* **1988**, *32*, 1. (d) Zarembowitch, J. *New J. Chem.* **1992**, *16*, 255.
(5) Decurtins, S.; Gütlich, P.; Hasselbach, K. M.; Spiering, H.; Hauser, A. *Inorg. Chem.* **1985**, *24*, 2174. Gütlich, P.; Hauser, A. *Coord. Chem. Rev.* **1990**, *97*, 1.
(6) Qi, Y.; Müller, E. W.; Spiering, H.; Gütlich, P. *Chem. Phys. Lett.* **1983**, *101*, 503.
(7) (a) Bousseksou, A.; Negre, N.; Goiran, M.; Salmon, L.; Tuchagues, J. P.; Boillot, M. L.; Boukheddaden, K.; Varret, F. *Eur. Phys. J. B* **2000**, *13*, 451. (b) Bousseksou, A.; Boukheddaden, K.; Goiran, M.; Consejo, C.; Boillot, M.-L.; Tuchagues, J.-P. *Phys. Rev. B* **2002**, *65*, 172412.
(8) Boillot, M. L.; Roux, C.; Audière, J. P.; Dausse, A.; Zarembowitch, J. *Inorg. Chem.* **1996**, *35*, 3975.

10.1021/cm0211406 CCC: $22.00
Published on Web 08/31/2002

Scheme 1. Ligand H_2(5-OMe-sal)$_2$trien

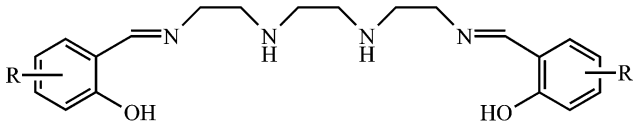

evidence of the crucial role played by co-intercalated water molecules on cooperativity.

Several groups have encapsulated or inserted spin-crossover species in various lattices, layered silicates,[9] zeolites,[10] and oxalates,[11] and even organized such molecules into Langmuir−Blodgett films.[12] Our group reported the continuous transition of a cationic $[Fe^{III}(sal\text{-}Een)_2]^+$ complex, inserted in the two-dimensional $CdPS_3$ host lattice and compared with that of the three-dimensional pure solid.[13]

The MPS_3 compounds (M = Mn, Fe, Cd, ...)[14] form a family of layered material that is known to react with solutions of many ionic salts G^+X^- to give intercalation compounds of the general formula $G_{2x}M_{1-x}PS_3\cdot(solvent)_y$.[15] In these compounds, the charge balance is maintained by the loss of one M^{2+} ion from the intralayer region for every two G^+ ions that are inserted in the interlayer region. When M is a paramagnetic ion (Mn, Fe), the pristine MPS_3 phases behave as antiferromagnets, but many intercalation compounds derived from these compounds acquire spontaneous magnetization[15] below a critical temperature. Therefore, $MnPS_3$ provides a magnetizable lattice suitable for submitting inserted species to a strong internal magnetic field or probing the ordering of the intercalated species. Along this line, we have recently shown that inserting photochromic spiropyrans in $MnPS_3$ gave rise to an unusual photomagnetic effect.[16]

The complex selected in the present work belongs to a family of Fe(III) chelates known for their ability to show spin crossover, particularly in solution.[17−20] These complexes containing hexadentate ligands [H_2-Rsal$_2$-trien] derive from triethylenetetramine and R-substituted salicylaldehydes where the aromatic rings can bear different substituents R (Scheme 1). The R substituent used in the present report is R = 5-OMe; thus the compound is formulated as $[Fe^{III}(5\text{-OMe-sal}_2\text{trien})]^+$.

Experimental Section

Synthesis of the Complex. $[Fe(5\text{-OMe-sal}_2\text{trien})]PF_6\cdot 0.5H_2O$ (hereafter denoted **1**) was prepared according to the procedure described by Wilson.[17] Elem Anal. ($FeC_{22}H_{28}O_4N_4PF_6\cdot 0.5H_2O$, M = 622 g mol^{-1}): Calcd: C, 42.44; H, 4.70; N, 9.00. Found: C, 42.22; H, 4.52; N, 8.83. We have refined the crystal structure of **1** at room temperature, the compound being at this temperature in the HS state. The molecular structure[21] compares with those[18,20] already described, and it will be published in a subsequent paper. There are minor differences in the NH groups of the ligand backbone which in this case are involved in two inequivalent hydrogen bonds with the PF_6^- anion (NH···F, 3.089 Å) and the water molecule (NH···O, 2.969 Å).

Synthesis of the $MnPS_3$ Intercalate. A two-step procedure was employed to insert the iron complex into $MnPS_3$: (i) A tetramethylammonium pre-intercalate $(Me_4N)_{2x}Mn_{1-x}PS_3$ was prepared by treating $MnPS_3$ (typically 200 mg) with Me_4NCl (1 g) in water (20 mL) at 20 °C for 1 h. After isolation, this intermediate compound (150 mg) was refluxed with an acetonitrile solution (5 mL) of $[Fe(5\text{-OMe-sal}_2\text{trien})]PF_6$ (200 mg) over 24 h. The solid compound was filtered and washed with acetonitrile until the filtrate become colorless. A dark-violet powder of the sought-for intercalate (denoted **2**) was obtained.

Measurements. X-ray powder diffraction patterns were recorded on a Siemens diffractometer using Cu Kα radiation. Infrared spectra of powders were obtained at room temperature on a FTIR Perkin-Elmer Spectrum 1000 spectrometer using KBr pellets (1:100).

Magnetic measurements were carried out on powdered samples of typical weight 15−20 mg using a Quantum Design SQUID magnetometer (MPMS5S model) operating between 4 and 300 K.

Thermogravimetric (TGA) analysis of the intercalate between 293 and 438 K was carried out using a Ugine-Eyraud zero balance. The heating rate was 2 K min^{-1} and the initial sample weight was 65 mg.

Mössbauer spectra were recorded on a constant-acceleration spectrometer, with a 25-mCi source of ^{57}Co in rhodium matrix. The polycrystalline absorber contained 30 mg of material per square cm. Variable-temperature spectra, in the 300−4 K range, were obtained by using a standard bath cryostat; the temperature was controlled by a linear sensor calibrated at 4.2 and 273 K. After folding of the spectra, the typical experimental line width, in the considered velocity range, was Γ_{exp} = 0.215 mm s^{-1}. The spectra were fitted without correction for the thickness effect. Least-squares-fitted parameters are given with their standard deviation of statistical origin (in parentheses), and isomer shift values refer to metallic iron at room temperature.

Results

Characterization of the Intercalate 2. The powder X-ray diffractogram of **2** (see Figure 1) shows very sharp 00*l* reflections (up to 007) corresponding to an interlayer spacing of 19.1 Å (6.5 Å for $MnPS_3$ and 11.5 Å for the NMe_4^+ intercalate). Full insertion of the complex was ascertained by the complete disappearance of the 001 reflection of the Me_4N intercalate at 11.5 Å. The diffractogram of **2** shows that this compound is *structurally* remarkably *well ordered*, despite the large size of the inserted cation. The first three 00*l* (l = 1, 2, 3) reflections are very intense and of nearly equal intensity.

(9) Nakano, M.; Okuno, S.; Matsubayashi, G. E.; Mori, W.; Katada, M. *Mol. Cryst. Liq. Cryst.* **1996**, *286*, 83.
(10) (a) Mizuno, K.; Lunsford, J. H. *Inorg. Chem.* **1983**, *22*, 3484. (b) Umemura, Y.; Minai, Y.; Koga, N.; Tominaga, T. *J. Chem. Soc., Chem Commun.* **1994**, 893.
(11) Sieber, R.; Decurtins, S.; Stoeckli Evans, H.; Wilson, C.; Yufit, D.; Howard, J. A. K.; Capelli, S. C.; Hauser, A. *Chem. Eur. J.* **2000**, *6*, 361.
(12) (a) Coronel, P.; Barraud, A.; Claude, R.; Kahn, O.; Ruaudel-Teixier, A. *J. Chem. Soc., Chem. Commun.* **1989**, 193. (b) Soyer, H.; Mingotaud, C.; Boillot, M. L.; Delhaes, P. *Langmuir* **1998**, *14*, 5890.
(13) Field, C. N.; Boillot, M. L.; Clément, R. *J. Mater. Chem.* **1998**, *8*, 283.
(14) (a) Klingen, W.; Ott, R.; Hahn, H. *Z. Anorg. Allg. Chem.* **1973**, *396*, 271. (b) Clément, R.; Garnier, O.; Jegoudez, J. *Inorg. Chem.* **1986**, *25*, 1404.
(15) Clément, R.; Léaustic, A. In *Magnetism: Molecules to Materials II. Molecule-Based Materials*; Miller, J. S., Drillon, M., Eds; Wiley-VCH: Weinheim, 2001; p 397.
(16) Bénard, S.; Leaustic, A.; Rivière, E.; Yu, P.; Clément, R. *Chem. Mater.* **2001**, *13*, 3709.
(17) Tweedle, M. F.; Wilson, L. J. *J. Am. Chem. Soc.* **1976**, *98*, 4824.
(18) (a) Sinn, E.; Sim, G.; Dose, E. V.; Tweedle, M. F.; Wilson, L. J. *J. Am. Chem. Soc.* **1978**, *100*, 3375. (b) Nishida, Y.; Kino, K.; Kida, S. *J. Chem. Soc., Dalton Trans.* **1987**, 1957.
(19) Dose, E. V.; Murphy, K. M. M.; Wilson, L. J. *Inorg. Chem.* **1976**, *15*, 2622.
(20) Maeda, Y.; Oshio, H.; Tanigawa, Y.; Oniki, T.; Takashima, Y. *Bull. Chem. Soc. Jpn.* **1991**, *64*, 1522.
(21) Floquet, S. Ph.D. Thesis. Université Paris-Sud, Orsay, France, 2001.

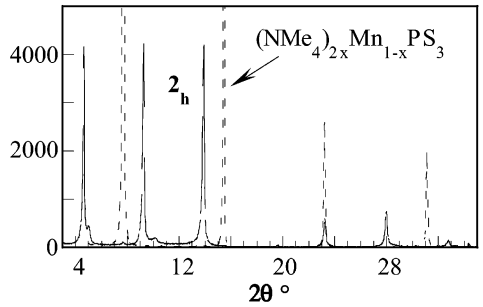

Figure 1. Powder X-ray diffraction spectra at room temperature of $\mathbf{2_h}$ and $(Me_4N)_{2x}Mn_{1-x}PS_3$.

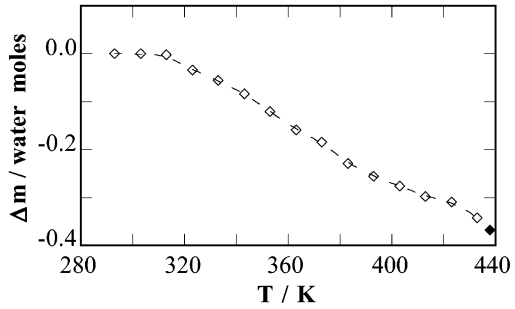

Figure 2. Weight loss versus temperature for $\mathbf{2_h}$ scaled as the equivalent number of water molecules.

Thermogravimetric analysis (TGA; see Figure 2) shows that **2** contains a small amount of co-intercalated water (2.2 wt %). The water molecules are released on heating over the temperature range 313−413 K. Upon standing overnight at room temperature under ambient atmosphere, 80% of the water loss is reinserted into the intercalate. In the following, the hydrated and anhydrous intercalates will be denoted $\mathbf{2_h}$ and $\mathbf{2_a}$, respectively.

Elemental analysis of $\mathbf{2_h}$ gives a formulation $[Fe(5\text{-}OMe\text{-}sal_2trien)]_{0.28}Mn_{0.86}PS_3 \cdot nH_2O$ (310.9 g mol^{-1}), where the amount of water is calculated from the TGA data. Calcd (n = 0.3): C, 23.79; H, 2.74; N, 5.04; P, 9.96; S, 30.94; Fe, 5.03; Mn, 15.19. Found: C, 24.37; H, 2.74; N, 5.19; P, 9.17; S, 30.80; Fe, 4.75; Mn, 15.33.

These data are consistent with an intercalation ratio of 0.28 mol of ferric complex per $Mn_{0.86}PS_3$ unit, which accounts for electric charge balance. It is worth noting that the amount of water reabsorbed by the dehydrated material $\mathbf{2_a}$ corresponds to one H_2O molecule per inserted molecule of complex. These H_2O species are most likely bonded to the Fe(III) complex by hydrogen bonds.

The IR spectra of $[Fe(5\text{-}OMe\text{-}sal_2trien)]PF_6 \cdot 0.5H_2O$ **1** and of intercalate $\mathbf{2_h}$ are shown in Figure 3. A number of peaks assigned to the ferric complex are obviously observed in the spectra of **1** and of $\mathbf{2_h}$. The peak due to the stretching mode of the phenolate CO group is located at 1295 cm^{-1} for **1** and at ≈1290 (sh)−1285 cm^{-1} for $\mathbf{2_h}$. The small peaks located at 3314 and 3284 cm^{-1} (**1**) or the broad peak at 3279 cm^{-1} ($\mathbf{2_h}$) are assigned to the NH stretching vibration mode. It can be inferred from these data that the nature of coordination core of the ferric cation remains unaltered after intercalation. As expected, the spectrum of $\mathbf{2_h}$ no longer exhibits the intense, broad band at 836 cm^{-1} due to the PF_6^- anion. On the other hand, the spectrum of $\mathbf{2_h}$ exhibits the

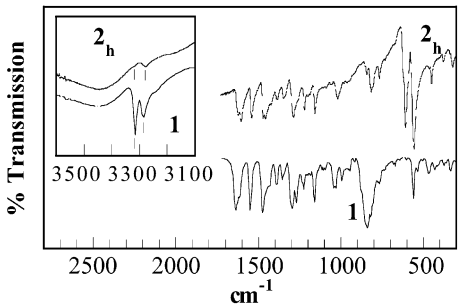

Figure 3. IRTF spectra of **1** and $\mathbf{2_h}$ at room temperature.

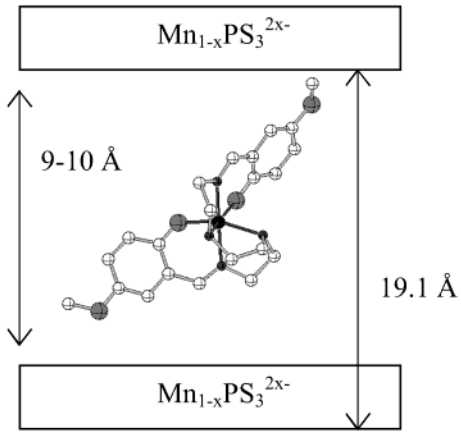

Figure 4. Schematic diagram of the cationic molecule **1** intercalated between the negatively charged layers of $Mn_{0.86}PS_3^{0.28-}$ $\mathbf{2_h}$.

intense $\nu(PS_3)$ stretching modes of $MnPS_3$, split into two components at 556 and 608 cm^{-1}. The presence of two sharp and well separated $\nu(PS_3)$ components constitute a characteristic feature that strongly suggests a *highly ordered* $Mn_{1-x}PS_3$ host lattice with one manganese vacancy close to each P_2S_6 group.[15]

All these data are therefore consistent with the presence in $\mathbf{2_h}$ of *nearly close-packed* $[Fe(5\text{-}OMe\text{-}sal_2trien)]^+$ cations lying in the interlayer galleries. The largest and smallest van der Waals dimensions of the HS guest species can be roughly estimated, from the X-ray diffraction data collected for the bulk sample, as 19 and 9−10 Å, respectively.[21] Therefore, the suggested orientation of the guest species lying with a tilt angle of 50° accounts well for the experimental basal spacing (19.1 Å), as shown schematically in Figure 4. We note that such an orientation leaves the N−H groups free to engage hydrogen bonds.

Magnetic Study. For the sake of comparison, the evolution of $\chi_M T$ (χ_M being the molar magnetic susceptibility) as a function of temperature was determined on a solid sample of $[Fe(5\text{-}OMe\text{-}sal_2trien)]PF_6 \cdot 0.5H_2O$ **1**. The $\chi_M T$ value of 4.33 cm^3 mol^{-1} K at 300 K, being almost temperature independent between 300 and 5 K, is characteristic of a ferric ion in a-HS ground state. This result contrasts with the thermal equilibrium ($T_{1/2} \approx$ 255 K, temperature at which this transition is halfway completed) reported for the anhydrous form of this complex in an acetone solution.[17]

The temperature dependence of the molar magnetic susceptibility of intercalate $\mathbf{2_h}$ is shown in Figure 5 as $1/\chi_M = f(T)$ per mole of $[Fe(5\text{-}OMe\text{-}sal_2trien)]_{0.28}Mn_{0.86}PS_3 \cdot nH_2O$ unit. Data recorded at increasing and de-

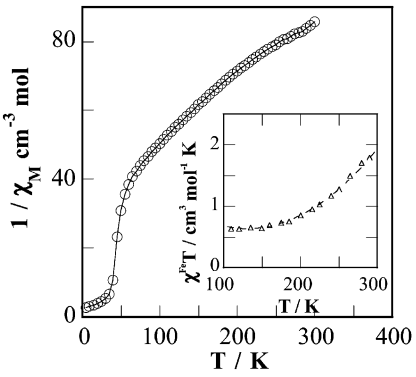

Figure 5. Temperature dependence of the inverse magnetic susceptibility $1/\chi_M$ for **2h** (χ_M being related to 1 mol of **2h**). Inset: Temperature dependence of $\chi^{Fe}T$ (χ^{Fe} being the magnetic susceptibility estimated for 1 mol of the inserted ferric complex).

creasing temperatures are strictly superimposable. Let us consider first the temperature region above 80−90 K. If nearly all $MnPS_3$ intercalates[15] known so far exhibit excellent agreement to a Curie−Weiss law above 80−90 K up to room temperature, in our case the plot obtained for **2h** displays a linear branch only from 80 to 150−160 K. The onset of negative curvature that appears above 170 K implies that the susceptibility of the compound (still referred to 1 mol of **2h**) rapidly increases in an unusual way. This behavior strongly suggests the onset of spin crossover of the inserted species. There is no theoretical expression available to describe accurately the magnetic data of intercalated $MnPS_3$. Therefore, with the purpose of extracting the minor magnetic contribution of the inserted iron complex from the experimental data dominated by the overwhelming contribution of the host lattice, we have tentatively assumed that the host lattice in **2h** was identical to the host lattice in the tetramethylammonium intercalate $(Me_4N)_{0.32}Mn_{0.84}PS_3$ which does contain a diamagnetic guest species and a comparable rate of manganese vacancies.[22] The result of this computation is shown in the inset of Figure 5 in the form of $\chi^{Fe}T$ versus T, where χ^{Fe} stands for the molar magnetic susceptibility originating solely from the inserted ferric complex. Although of qualitative value, the plot is consistent with a complex undergoing a spin-crossover process.

In the low-temperature region in Figure 5, non linearity of the intercalate $1/\chi_M(T)$ plot develops as the temperature is lowered, until below a critical temperature T_c a very large increase of the susceptibility is observed, indicating the onset of spontaneous magnetization. This low-temperature region (see Figure 6) has been studied using a very low field (30 Oe): (i) The field-cooled magnetization (FCM) actually displays a steep increase below $T_c \approx 36$ K. The field was then switched off at 10 K and the sample was allowed to warm up.

(22) By taking advantage of the existence of a Curie law both for the $MnPS_3$ layer and the ferric complex (from 80 to 150 K), one can estimate the product of the molar magnetic susceptibility of **2h** at high temperature by $\chi_M T = (1 - x)(\chi^{Mn}T) + 2x(\chi^{Fe}T)$. In this formula, x is the ratio of Mn vacancies ($x = 0.14$) and $1/\chi^{Mn} = aT + b$ represents the Curie law followed by related materials $C_{2x}Mn_{1-x}PS_3$, the slope ($a \sim 0.2424$ K^{-1}) being averaged over a set of data.[15] The iron ions are assumed to be in the LS state at 100 K, and the $\chi^{Fe}T$ values of the LS and HS species are taken as 0.5 ($\mu = 2\ \mu_B$) and 4.374 cm^3 mol^{-1} K ($\mu = 5.92\ \mu_B$), respectively.

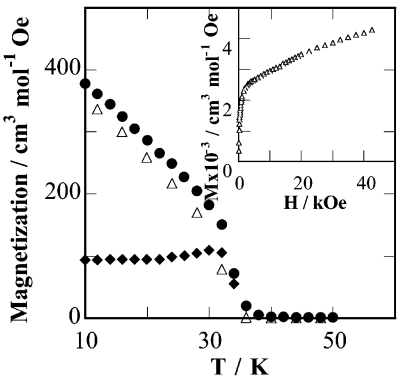

Figure 6. Temperature dependence of the field-cooled magnetization (●, FCM), remanent magnetization (△, RM), and zero-field-cooled magnetization (◆, ZFCM) of the **2h** intercalate in a field of 30 Oe. Inset: Dependence of the magnetization of **2h** on applied field at 10 K.

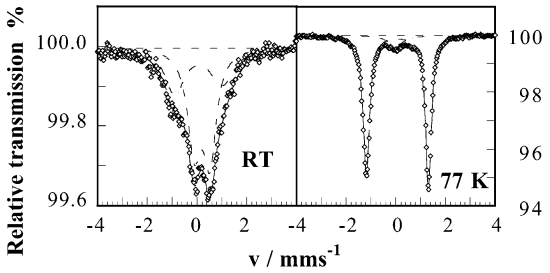

Figure 7. ^{57}Fe Mössbauer spectra of **2h** at 300 and 77 K. Measurements were performed at ambient atmosphere.

The remanent magnetization was quite strong, and it steadily decreased to vanish at T_c. The zero-field-cooled magnetization (ZFCM) was obtained by cooling from 100 to 10 K in zero field, then warming under 30 Oe. The ZFCM curve slightly increases on warming and drops rapidly at T_c.

Finally, the dependence of the magnetization vs applied magnetic field shown as an inset in Figure 6 has been measured at 10 K. M increases steeply at low applied field and above 10 Oe reaches a linear regime.

These data are characteristic of the occurrence of ferrimagnetism or weak ferromagnetism in **2h**, as occurs in many $MnPS_3$ intercalates below a critical temperature in the range 30−40 K, depending on the amount of manganese vacancies.[15]

Mössbauer study of the Intercalate. For the sake of clarity, the results are reported in two parts: a first one dealing with the spin crossover of the guest complex and a second one dealing with the para-/ferrimagnetic transition of the host and its influence on the Mössbauer spectrum of the inserted complex.

Spin Crossover of the Guest in the Paramagnetic Host. Mössbauer measurements have been performed as a function of temperature on the air-equilibrated sample **2h**, previously studied by a SQUID magnetometer. The absorption spectrum at 300 K and ambient atmosphere, displayed in Figure 7 (left), consists of the superposition of two absorption doublets assigned to HS ($\delta^{IS} = 0.338 \pm 0.007$ mm s^{-1}, $\Delta E_Q = 0.62 \pm 0.01$ mm s^{-1}) and LS ($\delta^{IS} = 0.198 \pm 0.000$ mm s^{-1}, $\Delta E_Q = 1.91 \pm 0.05$ mm s^{-1}) species, respectively. Decreasing the temperature to 77 K (Figure 7, right) results in opposite intensity variations of these doublets leading to a major LS component ($\delta^{IS} = 0.199 \pm 0.001$

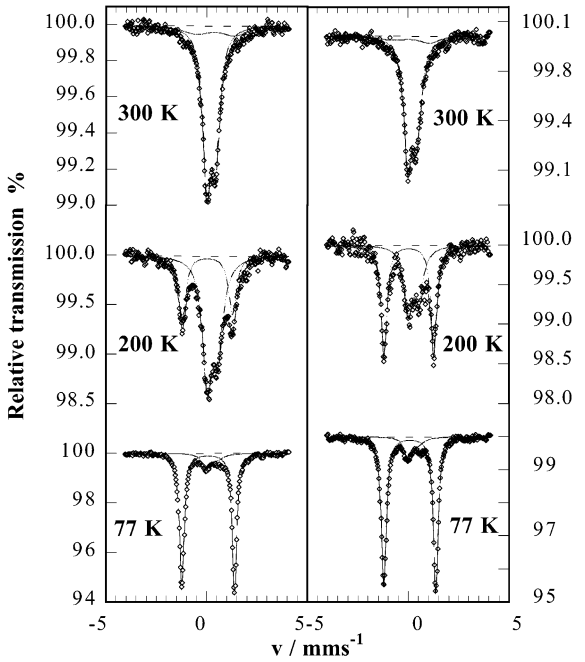

Figure 8. Selected Mössbauer spectra of $\mathbf{2_a}$ at 300, 200, and 77 K under dynamic vacuum. Measurements were performed in the cooling (left) and heating (right) modes.

mm s^{-1}, $\Delta E_Q = 2.49 \pm 0.01$ mm s^{-1}) and hence confirms the occurrence of a-HS to LS conversion.

These Mössbauer parameters are consistent with the data reported for some related complexes $[Fe^{III}(R_2\text{-trien})]X$ (R = acetylacetonate, salicylate, X = anion; δ^{IS}(HS) = 0.28−0.42 mm s^{-1} at room temperature, δ^{IS}(LS) = 0.14−0.23 mm s^{-1}, ΔE_Q(LS) = 2.23−2.97 mm s^{-1} at 120 K).[17−19] The HS fractions n_{HS} are estimated from the relative absorption area amount $a_{HS} = (A_{HS}/A_{tot})$ (A being the baseline-corrected area of the components) to ca. 0.60 (300 K) and 0.16 (77 K).

The sample was then heated from 77 to 300 K under a dynamic vacuum. At 250 K, a slow evolution of the absorption lines of the sample took place over several hours. A progressive variation of the area ratio a_{HS} from 0.38 to 0.60 after 1 day was observed. At this stage, when the temperature was raised to 275 K, no further evolution could be detected over time, suggesting that the slow transformation of $\mathbf{2_h}$ was complete. Anticipating the discussion, $\mathbf{2_h}$ has turned into the dehydrated form $\mathbf{2_a}$ at this stage. After return to 300 K under vacuum, the Mössbauer spectra of the sample $\mathbf{2_a}$ reexposed to air (denoted $\mathbf{2_{rh}}$) was recorded. Then, the anhydrous form $\mathbf{2_a}$ was again re-formed by pumping and its absorption spectrum was recorded over a new cycle of temperature under vacuum. Figure 8 shows a set of selected spectra of $\mathbf{2_a}$ at 300, 200, and 77 K. The least-squares-fitted parameters for the different forms of the sample ($\mathbf{2_h}$, $\mathbf{2_a}$, and $\mathbf{2_{rh}}$) are collected in Table 1. The data obtained for $\mathbf{2_{rh}}$ repumped under vacuum at 300 K and those for $\mathbf{2_a}$ are not distinguished as the sets of parameters for both samples at different temperatures are found to be identical.

The main features observed for $\mathbf{2_a}$ at 300 K are (i) a prevailing asymmetric HS doublet ($\delta^{IS} = 0.33 \pm 0.01$ mm s^{-1}) with a value of a_{HS} close to unity (0.88), (ii) a different quadrupolar splitting value ($\Delta E_Q = 0.45 \pm 0.01$ mm s^{-1}), and (iii) an asymmetry of the line intensity opposite the one of the air-equilibrated sample $\mathbf{2_h}$. From the comparison of the data obtained for $\mathbf{2_h}$ and $\mathbf{2_a}$, it appears that varying the temperature between 300 and 77 K resulted in different HS ↔ LS transformations as illustrated by the variation of the relative area of both components (see Figure 9). The whole set of data for sample $\mathbf{2_a}$ (cooling mode and subsequent heating mode) provides evidence for a hysteresis loop. The observation of two resolved contributions indicates that the spin interconversion rates are slow compared to the hyperfine frequencies (ca. 10^8 s^{-1}).

The thermal dependence of the HS fraction n_{HS} was readily determined from the variation of the area ratio $a_{HS} = (A_{HS}/A_{tot}) \approx n_{HS}$ because the differences between Lamb−Mössbauer factors of both spin states analyzed from $Ln(A_{tot})$ vs temperature[23] are very small.

The values of the Debye temperature and effective mass, which provide some insight into the vibrational modes of the ferric atom and the lattice, were obtained through the analysis of the isomeric shift and absorption data by the Debye model of the lattice dynamics.[23] The thermal dependence of δ^{IS} is a decreasing function of the temperature as expected from the second-order Doppler effect. The slope of δ^{IS}(LS) (77 and 160 K) is equal to -2.287×10^{-4} mm s^{-1} K^{-1}, which corresponds to a LS effective mass of 182 atomic mass units.[24] This value, much larger than the atomic one (^{57}Fe), reveals a strong binding of the metal atom to its surroundings. A rather low LS Debye temperature of ca. 83 K for the lattice properties was also found.

The analysis of the thermal dependence of the quadrupole splitting parameters reveals almost temperature-independent behaviors except, for the LS state, in the range where the spin transition takes place. This might indicate that the excited states arising from a local symmetry lower than cubic may be thermally populated in the temperature range of the transition. However, the decrease of LS quadrupole splitting at high temperature might be due to an alternative explanation: the presence of a dynamic mixing of the HS and LS absorption lines. In such a case, the LS line width should vary with the HS fraction that is indeed observed. However, the corresponding HS quadrupole splitting should also vary, while it is found to be almost unaffected. This discrepancy might be accounted for by the combination of several effects.

LS Guest−Ferrimagnetic Host. At 40 K the Mössbauer spectrum is characterized by the two quadrupolar components of the prevailing LS ferric ion with those of a small amount of Fe(III) species trapped in the HS state ($n_{HS} \approx 0.12 \pm 0.02$ at 77 K). The main finding at 4.2 K consists of an $S = 1/2$ quadrupolar doublet showing marked intensity and line-width asymmetries. The fitted parameters of the $S = 1/2$ absorption line are $\delta^{IS} = 0.193 \pm 0.001$ mm s^{-1} and $\Delta E_Q = 2.469 \pm 0.003$ mm s^{-1}.

Discussion

Although several examples of spin crossover in intercalated or inserted systems have been reported, no

(23) *Mössbauer spectroscopy*; Greenwood, N. N., Gibb, T. C., Eds.; Chapman and Hall Ltd.: London, 1971; pp 11, 52.
(24) Oshio, H.; Kitazaki, K.; Mishiro, J.; Kato, N.; Maeda, Y.; Takashima, Y.; *J. Chem. Soc., Dalton Trans.* **1987**, 1341.

Table 1. Selected ^{57}Fe Mössbauer Fitted Parameters of [Fe((5-OMe-sal)$_2$trien)]$_{0.28}$Mn$_{0.86}$PS$_3$·*n*H$_2$O in Different States[a]

	T, K	$\delta^{IS}(^2T_2)$, mm·s^{-1}	$\Delta E_Q(^2T_2)$, mm·s^{-1}	$\Gamma^-(^2T_2)$, mm·s^{-1}	$\Gamma^+(^2T_2)$, mm·s^{-1}	$\delta^{IS}(^6A_1)$, mm·s^{-1}	$\Delta E_Q(^6A_1)$, mm·s^{-1}	$\Gamma^-(^6A_1)$, mm·s^{-1}	$\Gamma^+(^6A_1)$, mm·s^{-1}	Ln (A_{tot})	n_{HS} (0.02)
2$_h$	300	0.198(0)	1.91(5)	0.94(4)	1.19(3)	0.338(7)	0.62(1)	0.61(1)	0.66(1)	0.250	0.60
2$_h$	77	0.199(1)	2.49(1)	0.28(1)	0.30(1)	0.428(0)	0.60(0)	0.80(3)		1.604	0.16
2$_{(*)}$	190	0.172(2)	2.47(1)	0.31(1)	0.32(1)	0.308(0)	0.59(0)	0.58(1)	0.89(1)	0.914	0.18
2$_{(*)}$	220	0.158(2)	2.43(1)	0.39(1)	0.40(1)	0.30(1)	0.58(2)	0.49(1)	0.59(1)	0.717	0.23
2$_{(*)}$	250	0.148(7)	2.32(1)	0.59(1)	0.62(1)	0.37(1)	0.52(1)	0.63(1)	0.76(1)	0.594	0.60
2$_{(*)}$	300	0.24(1)	1.89(4)	1.14(2)	2.06(3)	0.32(1)	0.43(1)	0.44(1)	0.54(1)	0.384	0.85
2$_{rh}$	300	0.169(2)	2.09(3)	0.70(3)	0.96(3)	0.31(1)	0.63(1)	0.82(1)	0.92(2)	0.326	0.72
2$_a$	300	0.184(2)	2.14(1)	0.64(1)	0.98(1)	0.33(1)	0.45(1)	0.48(1)	0.58(1)	0.378	0.88
2$_a$	245	0.157(2)	2.45(4)	0.58(3)	0.58(3)	0.36(1)	0.47(1)	0.60(1)	0.68(3)	0.632	0.86
2$_a$	200	0.162(4)	2.48(1)	0.475(1)	0.433(1)	0.40(1)	0.50(1)	0.54(1)	0.70(1)	0.827	0.67
2$_a$	160	0.172(1)	2.57(1)	0.271(1)	0.277(1)	0.36(1)	0.56(1)	0.44(1)	0.66(1)	1.03	0.27
2$_a$	77	0.189(1)	2.58(1)	0.284(1)	0.292(1)	0.29(2)	0.48(3)	0.38(2)	0.74(5)	1.46	0.12
2$_a$	160	0.170(1)	2.55(1)	0.280(2)	0.289(2)	0.35(1)	0.52(2)	0.46(1)	0.74(3)	0.99	0.24
2$_a$	200	0.151(3)	2.47(1)	0.360(1)	0.340(6)	0.37(1)	0.52(1)	0.40(1)	0.60(2)	0.776	0.43
2$_a$	240	0.147(4)	2.35(1)	0.488(8)	0.464(8)	0.36(1)	0.54(1)	0.62(1)	0.78(1)	0.627	0.58
2$_a$	260	0.170(1)	2.31(3)	0.800(3)	0.580(2)	0.37(1)	0.49(1)	0.56(1)	0.68(1)	0.504	0.74
2$_a$	300	0.24(1)	1.89(4)	1.14(2)	2.06(3)	0.32(1)	0.43(1)	0.44(1)	0.54(1)	0.384	0.85
2$_h$	4.2	0.193(1)	2.469(3)	0.468(2)	0.600(2)					1.86	*0*
2$_{(*)}$	15.5	0.192(1)	2.479(2)	0.292(2)	0.376(2)					1.69	*0*
2$_a$	25	0.189(1)	2.499(2)	0.300(2)	0.374(2)					1.78	*0*
2$_{(*)}$	30	0.192(1)	2.474(2)	0.282(2)	0.320(2)					1.69	*0*
2$_{(*)}$	35	0.192(1)	2.478(2)	0.278(2)	0.298(2)					1.77	*0*
2$_a$	45	0.190(1)	2.495(2)	0.282(1)	0.306(2)					1.70	*0*
2$_{(*)}$	65	0.189(1)	2.480(1)	0.280(1)	0.294(1)					1.66	*0*

[a] **2$_{(*)}$** stands for **2$_h$** under dynamic vacuum, and **2$_{rh}$** denotes a rehydrated sample formed by exposure of **2$_a$** to the ambient air. Isomer shifts are relative to Fe metal. Italic values were fixed in fitting. A_{Tot} is the normalized absorption area. Γ^- and Γ^+ are the line widths of the thinnest and thickest quadrupole lines, respectively.

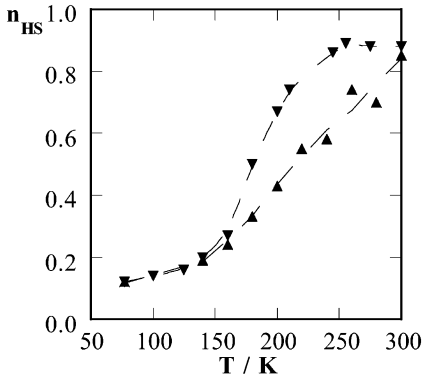

Figure 9. Temperature dependence of the HS fraction for compound **2$_a$** deduced from the fractional area of the Mössbauer components, $n_{HS} \approx A_{HS}/A_{tot} = a_{HS}$.

hysteresis effect has been evidenced so far, except for a Langmuir−Blodgett film.[12a] In this context, the most intriguing features shown by the present data are the occurrence of a discontinuous transition with a thermal hysteresis for **2$_a$** and a mere continuous transition for the hydrated form **2$_h$**.

The slow evolution of the Mössbauer spectrum of **2$_h$**, observed at 250 K under dynamic secondary vacuum, has been ascribed to the loss of the co-intercalated water molecules and hence to the formation of the anhydrous compound **2$_a$**. Actually, TGA shows that the dehydration reaction **2$_h$** → **2$_a$** is easily achieved under mild conditions. The subsequent rehydration of **2$_a$** is also identified from the Mössbauer measurements. Indeed, when the dehydrated sample **2$_a$** is exposed to air, reinsertion of water results at least partly into the opposite **2$_a$** → **2$_{rh}$** reaction as shown by the change of both the HS fraction (n_{HS} = 0.88 (**2$_a$**) and 0.72 (**2$_{rh}$**)) and the quadrupolar splitting values (ΔE_Q = 0.45 (**2$_a$**) and 0.63 mm s^{-1} (**2$_{rh}$**)) and the concomitant inversion of the HS doublet asymmetry.

As the physical conditions required to form **2$_h$** (ambient atmosphere or a low pressure with static helium gas as in the SQUID magnetometer) and **2$_a$** (cryogenic pumping, $p \sim 10^{-6}$ Torr) are very different, the direct comparison of the magnetic properties of **2$_a$** and **2$_h$** is not straightforward. We have performed magnetic susceptibility measurements on a solid sample introduced into a quartz sample holder and measured before (a) and after (b) a treatment under vacuum ($p \sim 10^{-2}$ Torr, 300 K, 48 h), the sample holder being sealed at this stage. For this sample maintained under primary vacuum (b), the transition curve presents characteristics different from those of the hydrated (**2$_h$**) and anhydrous samples (**2$_a$**), the main features being the absence within the experimental error of any hysteresis effect and a $\chi_M T$ value (∼3.71 cm^3 mol^{-1} K) at 300 K larger than $\chi_M T$(**2$_h$**) (∼3.50 cm^3 mol^{-1} K) and smaller than the value calculated (∼3.92 cm^3 mol^{-1} K) from the Mössbauer data of **2$_a$**. As the solid samples studied in Mössbauer and SQUID experiments are identical, the absence of hysteresis is ascribed to the fact that the sample is not dehydrated enough under the SQUID condition (b). These observations are also in qualitative agreement with the Mössbauer data as the $\chi_M T$ value at RT increases (decreases) when sample **2$_h$** is dried under vacuum (exposed to air).

Removing water from a spin-crossover solid usually leads to the loss of hydrogen-bonding interactions with complexes,[1,25] and therefore to the relative stabilization of one of the spin states of the metal ion. For the molecules of the type [Fe^{III}(Rsal$_2$trien)]X, the influence of solvent−solute interactions on the spin equilibria is

(25) Greenaway, A. M.; O'Connor, C. J.; Schrock, A.; Sinn, E. *Inorg. Chem.* **1979**, *18*, 2692.

well documented. As the electronic density on the nitrogen atom and consequently the metal−ligand interaction are reinforced by such hydrogen bonds,[17,26] it can be inferred that the removal of water molecules should cause the ligand field parameter to decrease and favor the HS state, a conclusion consistent with the data. Beyond the mere variation of the HS fraction and the shift of the transition temperature, it should be emphasized that the water species also controls the appearance/disappearance of a hysteresis effect.

Indeed the most striking result for compound **2a** (see Figure 9) is the occurrence of a thermal hysteresis, characterized by an asymmetrical and broad shape, centered at $T_{1/2} \approx 210$ K ($T_{1/2}\downarrow \approx 189$ K and $T_{1/2}\uparrow \approx 232$ K in the cooling and heating modes, respectively). The hysteresis loop is repeatedly observed after carrying out successive thermal cycles, provided that the compound is kept under vacuum. The spin transformation is complete neither at room temperature ($n_{HS} \approx 0.90$ at 300 K) nor at low temperature. Comparison of the data obtained at 77 K for intercalates **2h** and **2a** does not allow us to detect a significant difference of the residual HS fraction (the fraction of ferric complexes remaining in the HS state) evaluated as $n_{HS} \approx 0.12$. As already pointed out for a similar material,[13] these residual HS species are likely to result from the existence of a small amount of structural defects in the solid phase.[2,27]

The magnetic behavior of intercalate **2a** showing up a hysteresis effect contrasts with the properties usually reported in the literature. Let us examine the characteristics of this compound that could be related to cooperativity. From the powder X-ray diffraction data, it has been shown that this compound consists of homogeneously spaced host−guest layers and therefore presents some long-range ordering. An important structural feature of the intercalation compounds formed in the MPS_3 family is that the guest molecules are always densely packed within the interlamellar space. In the present case, for instance, assuming guest molecules shaped as "van der Waals cylinders" tilted by 50° with respect to the MPS_3 sheets, the area of the projection of the molecular cross section onto the layer plane compares with the area of the $MnPS_3$ unit cell (51.1 Å^2 per 1.12 Fe complexes and 64 Å^2 per $2P_2S_6$ units). The dense packing is a crucial feature of the intercalate, because the mean metal−ligand distances of such ferric complexes[28] significantly vary in the course of the spin crossover ($\Delta r = 0.12-0.15$ Å) and therefore the related change of volume of the complex leads to a variation of the unit cell volume exceeding the thermal expansion of the solid lattice. Such changes of volume must induce some local stresses (compression or tension) that have to be accommodated by the lattice according to the elastic properties of the solid. Following the theoretical and experimental analysis of Spiering, the elastic interactions contribute to the cooperative character of the spin crossover through (i) the long-range contribution in the form of an image pressure, (ii) a direct interaction due to the strain field between molecules, and (iii) the change of elastic self-energy due to the anharmonicity of the crystal.[29,30] The magnetic properties of a number of mixed-crystal[31] or ground spin-crossover compounds[27] have been rationalized by these effects.

As a consequence of the strong anisotropy of the intercalate presently studied (alternating guest and $MnPS_3$ layers **2a**), these effects can either primarily take place within the molecular layers or involve interlayer contributions. In the first case, the cooperative character of this transition is mainly due to the specific guest organization in a two-dimensional packing in conjunction with a highly ordered material. In the second case, additional elastic interactions should be associated with significant interlayer spacing modifications.

Let us first consider the present intercalate at low temperature. The LS molecules of smaller size are close packed between $MnPS_3$ layers. The formation of a few individual HS molecules of larger size requires the system to overcome the macroscopic strains imposed by the LS guest−host lattice, and therefore the isolated HS molecules should experience positive image pressures. It seems reasonable to assume that, at high temperature, the expanded HS guest−host lattice system does not impose the same constraints and energy barriers for the transformation of individual molecules. Indeed, the HS → LS conversion begins with the formation of a few individual LS species which are submitted to a negative image pressure from the whole system.

Elastic interactions, arising from long-range and direct intermolecular couplings, are responsible for the cooperative character of the LS ↔ HS transformation. Their strength can be inferred from the presence of a rather wide thermal hysteresis. From the variations of the interlayer spacing of some photoactive $MnPS_3$ intercalates[16] (ca. 0.2 Å), such a mechanism based on a three-dimensional cooperativity cannot be disregarded for this material.

As pointed out by König,[2] the appearance of a hysteresis loop spreading out over a large range of temperature can be attributed to the presence of defects and/or a particle size effect. Both of them are responsible for a reduction of the domain size and hence bent shape of the hysteresis loop. This is consistent with the rather large size dispersion of the studied crystallites that has been found to be larger than 15−635 μm.

The question which now arises is why the presence of co-intercalated water in **2h** destroys the cooperativity to such an extent that hysteresis is suppressed. This finding raises the question of how a solvate molecule may affect the transformation. Water insertion is accompanied by the formation of hydrogen bonds between water and cation molecules, which very likely modify the nature and the strength of the interactions between these molecules. As hydration of the sample reduces the cooperative interactions, it can be suggested that the solvent molecule plays a prevailing role of a spacer between molecules. An alternative explanation is based

(26) Zhu, T.; So, C. H.; Schaeper, D.; Lemke, B. K.; Wilson, L. J. *Inorg. Chem*. **1984**, *23*, 4345.
(27) Haddad, M. S.; Federer, W. D.; Lynch, M. W.; Hendrickson, D. N. *Inorg. Chem*. **1981**, *20*, 131.
(28) Timken, M. D.; Hendrickson, D. N.; Sinn, E. *Inorg. Chem*. **1985**, *24*, 3947.
(29) (a) Jung, J.; Schmitt, G.; Wiehl, L.; Hauser, A.; Knorr, K.; Spiering, H.; Gütlich, P. *Z. Phys. B* **1996**, *100*, 523. (b) Jung, J.; Bruchhäuser, F.; Feile, R.; Spiering, H.; Gütlich, P. *Z. Phys. B* **1996**, *100*, 517.
(30) Wiehl, L.; Spiering, H.; Gütlich, P.; Knorr, K. *J. Appl. Crystallogr*. **1990**, *23*, 151.
(31) (a) Sorai, M.; Ensling, J.; Gütlich, P. *Chem. Phys*. **1976**, *18*, 199. (b) Martin, J. P.; Zarembowitch, J.; Bousseksou, A.; Dworkin, A.; Haasnoot, J. G.; Varret, F. *Inorg. Chem*. **1994**, *33*, 6325.

on the introduction of defects associated with the water insertion. Indeed, König et al. have shown how a first-order transition with a hysteresis effect may be transformed into a quasi-continuous transition by introducing structural defects.[2,32] It is also well established that solvent-containing compounds present additional defects due, for example, to vacancies, position, or orientational disorder. In conclusion, it is suggested that the observed changes between the thermodynamic behaviors of $\mathbf{2_h}$ and $\mathbf{2_a}$ can be accounted by (i) the modification of intermolecular interactions and/or the loss of some long-range order arising from a number of positional and orientational defects due to water and (ii) the inductive effects arising from hydrogen bonds.

The Magnetically Ordered Region below 35 K. Let us consider now the temperature region where the intercalate $\mathbf{2_a}$ acquires a spontaneous magnetization. In the paramagnetic phase, the internal magnetic field due to the host lattice is zero in a first approach and the Mössbauer spectra show the quadrupolar components of the LS ferric ion in addition to those of the residual HS species. More precisely, in the present case, the fluctuations of the electron spin are not perfectly fast with respect to the Mössbauer time scale ($\sim 10^{-8}$ s), and a sizable asymmetrical line broadening is observed. In the ferrimagnetic phase ($T \leq T_c = 36$ K), the internal magnetic field arising from the spin ordering within the $MnPS_3$ layer does not produce any resolved magnetic splitting of the above-described spectra. However, the Mössbauer spectra collected at $T < T_c$ present an obvious enhancement of the marked intensity and line-width asymmetries of the LS quadrupole doublet. The HS contribution is no longer visible, probably due to similar magnetic perturbation, then acting on a larger spin, combined with the huge anisotropic character of the magnetic hyperfine tensor, which usually tends to smear the HS ferrous lines in nonstoichiometric compounds.[33] The low-temperature broadening of the quadrupole lines is shown in Figure 10, where the line-width difference $\Delta\Gamma = \Gamma^+ - \Gamma^-$ is plotted as a function of temperature. The correlation between the magnetic ordering of the system and the sharp increase in $\Delta\Gamma$ is obvious. The mechanism of the broadening effect may be the static effect of the net magnetization of the $MnPS_3$ layers; in addition, the slowing of the electronic spin relaxation may take place, due to the magnetic ordering as previously described for an hybrid organometallic−inorganic layered material.[34]

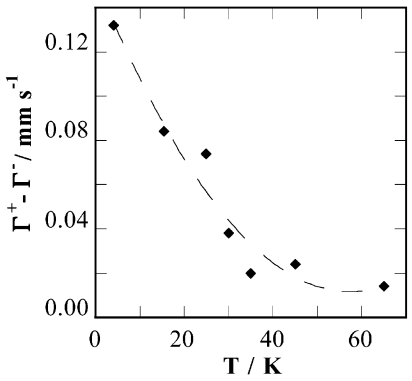

Figure 10. Line-width difference $\Delta\Gamma = \Gamma^+ - \Gamma^-$ versus temperature for the LS quadrupole doublet of $\mathbf{2_a}$ in the range 4−70 K.

Conclusion

A layered material of $MnPS_3$ intercalated with a cationic iron(III) chelate has been shown to exhibit both the thermal spin crossover of the guest molecule and a ferrimagnetic ordering of the host lattice. In the high-temperature range, two types of spin-crossover processes have been evidenced—a spin equilibrium and a transition with a thermal hysteresis—depending on whether the guest molecule is hydrated or anhydrous. The more or less cooperative character of the transition is analyzed in terms of elastic interactions due to the structural characteristics of these compounds (structural role of the $MnPS_3$ layers) and the possible modification of the cooperative interactions and/or the introduction of defects. In the low-temperature range where the low-spin state of the guest molecule is stabilized, the magnetization resulting from the ferrimagnetic ordering of the host lattice is detected. The internal magnetic field caused by the $MnPS_3$ layers is not strong enough to result in a magnetic hyperfine splitting of the LS Mössbauer absorption. However, it has been shown that a spin polarization effect due to this magnetic field is responsible for a significant broadening of the Mössbauer lines of the LS doublet. The nature of the intercalated molecules does not significantly influence the T_c value of the ferri-/paramagnetic transition.

Further studies are suggested, taking advantage of the high T_c value of such ferrimagnetic intercalated materials (with respect to the temperature range of usual spin-crossover processes): the possible interplay between the overall magnetization of the material and (i) the photoinduced spin conversion (LIESST or LD-LISC process)[5,8] and (ii) the relaxation rate of the metastable state (which recently was shown to be sensitive to external magnetic field).[35]

Acknowledgment. We thank Jean-Paul Audière for TGA measurements. This work was financially supported by the European Union within a TMR network (ERB-FMRX-CT98-0199).

CM0211406

(32) König, E.; Ritter, G.; Irler, W.; Goodwin, H. A. *J. Am. Chem. Soc.* **1980**, *102*, 4681.

(33) Ferey, G.; de Pape, R.; Varret, F. *J. Phys. (Fr.)* **1977**, *38*, C-7, 107.

(34) Coronado, E.; Galan-Mascaro, J.-R.; Gomez-Garcia, C.-J.; Ensling, J.; Gütlich, P. *Chem. Eur. J.* **2000**, *6*, 552.

(35) Koshihara, S.; Ogawa, Y.; Ishikawa, T.; Boukheddaden, K.; Varret, F. Submitted for publication in *Phys. Rev. Lett.*